CONFIDENTIAL



NACA RM E51L19

NACA

# RESEARCH MEMORANDUM

## INVESTIGATION AT MACH NUMBER 1.91 OF SPREADING CHARACTERISTICS OF JET EXPANDING FROM CHOKED NOZZLES

By Morris D. Rousso and L. Eugene Baughman

Lewis Flight Propulsion Laboratory
Cleveland, Ohio





RM E51L19

NATIONAL ADVISORY COMMITTEE FOR AERONAUTICS

WASHINGTON

February 11, 1952

CONFIDENTIAL

NATIONAL ADVISORY COMMITTEE FOR AERONAUTICS

RESEARCH MEMORANDUM

# INVESTIGATION AT MACH NUMBER 1.91 OF SPREADING CHARACTERISTICS OF JET EXPANDING FROM CHOKED NOZZLES

By Morris D. Rousso and L. Eugene Baughman



## SUMMARY

An investigation at Mach number 1.91 was made to determine by means of total-temperature surveys the gross spreading characteristics of jets expanding from convergent and convergent-divergent nozzles in the base of a body of revolution with various boattail configurations. The surveys were made in the region from the nozzle exit to a station 8 nozzle diameters downstream for nozzle pressure ratios from 2.5 to 16.0.

A comparison of temperature profiles of a jet expanding into a supersonic air stream with those of a jet expanding into quiescent air showed a considerable decrease in jet size for the jet in a moving stream. This decrease ranged from approximately 37 percent at an axial station of 1 diameter downstream of the nozzle exit to more than 55 percent at 8 diameters and was accounted for in part by the fact that the static pressure in the immediate vicinity of the nozzle exit was greater than the free-stream static pressure because of the strong trailing shock which resulted in a lower effective pressure ratio. In addition, the decreased relative motion between the jet and moving stream caused a smaller jet wake because of decreased mixing.

The effects of afterbody geometry on the jet wake were small. Changing the angle of the boattail had no appreciable effect on jet size; however, changing from a completely boattailed to a partially boattailed configuration resulted in a slightly larger jet.

The jet expanding from a convergent-divergent nozzle gave slightly larger jet profiles than the jet expanding from a convergent nozzle at the same overpressure ratio.

## INTRODUCTION

One of the problems confronting designers of supersonic and transonic airplanes and missiles is the damaging effects to the aircraft surfaces due to heating and buffeting by the expanding jets. In order to insure that these surfaces are not exposed to the jet, a knowledge

of the rate of spread and decay of jets under various conditions is required.

Some answers to this problem have been obtained from a research program at the NACA Lewis laboratory, wherein studies have been made to determine the characteristics of the jet wakes in quiescent air by means of temperature surveys (references 1 and 2) and total-pressure surveys (references 2 and 3). The results of this program are thus generally applicable only to the conditions of take-off and perhaps low flight speeds. For this reason an additional phase of the jet spreading program was included which undertook, by means of temperature surveys, to define a heated jet expanding into an air stream of Mach number 1.91.



The model through which the jet discharged was a body of revolution having a conical forebody and afterbody. Jets from both a convergent and a convergent-divergent nozzle were investigated for a range of nozzle-pressure ratios, for two boattail angles, and for two ratios of base to body diameter.

## SYMBOLS

The following symbols are used in this report:

$D_b$ base diameter of body (in.)

$D_m$ maximum diameter of body (in.)

M Mach number

$M_j$ theoretical jet Mach number, $\left\{\frac{2}{\gamma-1}\left[\left(\frac{P_p}{p_0}\right)^{\frac{\gamma-1}{\gamma}} - 1\right]\right\}^{\frac{1}{2}}$

P total pressure

p static pressure

R radial distance from jet center line, (nozzle diam)

T total temperature

U velocity of air at outer edge of boundary layer

u local velocity of air in boundary layer

X distance along thermocouple rake from jet center line, (nozzle diam)

Y lateral distance of rake from jet center line, (nozzle diam)

Z axial distance downstream of nozzle exit, (nozzle diam)

$\gamma$ ratio of specific heats

$\delta$ thickness of boundary layer at $u = U$

$\varepsilon$ angle between boattail surface and body axis (deg)

$\theta$ dimensionless temperature ratio, $\frac{T - T_0}{T_p - T_0}$

Subscripts:

0 ambient

p nozzle inlet

## APPARATUS AND PROCEDURE

The apparatus (fig. 1) consisted of a strut-mounted body of revolution having interchangeable afterbodies. The heated jet air entered the body through the passages in the strut, was turned 90° in the center body, and after passing through a straightening screen was discharged from the nozzle. In the final model configuration a second dummy strut (fig. 2) was located diametrically opposite the support strut for reasons which will be discussed later.

The assembled body of revolution had an over-all length of $20\frac{1}{2}$ inches and a fineness ratio of $10\frac{1}{4}$. Both the nose and the boattail (afterbody) were conical in shape and the center portion of the model was cylindrical. Boattail angles of 5.63° and 9.33° were used, the values of the ratio of base to body diameter were 0.385 and 0.525 (see fig. 3), and the ratio of nozzle exit to body diameter was constant at 0.375. The convergent-nozzle profile was contoured for a constant Mach number gradient based on one-dimensional considerations. The convergent-divergent nozzle was designed by the method of characteristics.

The high-pressure service air passed through two 15,000-watt circular resistance-type electric heaters prior to passing through the model. Throttling of the service air provided variation of jet-pressure ratio while the temperature of the air at the nozzle exit was held constant at 300° F by automatic temperature controls.

The average jet total pressure was measured by a single calibrated pitot tube located at a point near the nozzle entrance, whereas the jet total temperature was measured with a shielded total-temperature thermocouple mounted in the upstream portion of each nozzle. The external surfaces of the boattails were instrumented with static-pressure orifices and the divergent portion of each convergent-divergent nozzle was instrumented with a row of 11 static-pressure orifices. The nozzle pitot tube and internal static orifices were connected to a mercury manometer board, whereas all external body static orifices were connected to a dibutylphthalate manometer board, which was read visually to $\pm 0.02$ inch. All static-orifice diameters were 0.015 inch.



Temperatures in the jet wake were measured by a traversing thermocouple rake. The thermocouple rake was calibrated in the 18- by 18-inch supersonic wind tunnel in which the minimum recovery of each thermocouple was 98.5 percent. In addition, a single temperature probe was utilized to check the validity of data obtained with the rake. Figure 4, in which temperature coefficient $\theta$ is plotted as a function of radial distance from the jet center, shows that the jet profiles determined by both techniques are the same.

Boundary-layer thickness at the base of the model was obtained from total pressures measured by means of a movable pitot tube mounted on a streamlined support (fig. 2). A ring was placed near the tip of the nosepiece as a means of artificially inducing transition to turbulent flow and thereby assuring reproducible boundary-layer thickness for every run.

The test facility used for the investigation was the 18- by 18-inch supersonic wind tunnel (Mach number 1.91) at the NACA Lewis laboratory. Test-section total temperature and pressure were approximately $150^{\circ}$ F and atmospheric, respectively. The Reynolds number in the test section was approximately $3.24 \times 10^6$ per foot. The dew point was maintained within the range from $-10^{\circ}$ to $3^{\circ}$ F.

## RESULTS AND DISCUSSION

### Preliminary Development

Initial runs with the model supported by a single strut indicated appreciably asymmetrical flow at the base of the body. This asymmetry was evidenced by nonuniform pressures and boundary layer on the boattail as well as by displacement of the jet center line from the body axis. For these reasons a dummy strut was located diametrically opposite the support strut with a resulting symmetry in two planes and hence greater over-all symmetry. Schlieren photographs of the flow in the vicinity of the body base with single and double struts are shown in figure 5 to illustrate this point.

Inasmuch as the spreading characteristics of the jets are a function of the mixing between the jet and the stream, it was necessary to define the boundary layer at the end of the afterbody. Thus, boundary-layer profiles were determined at the base in the plane of the support strut as an indication of the initial conditions of the external stream before mixing. Boundary-layer profiles for various jet-pressure ratios are shown in figure 6. The afterbody used for this investigation was completely boattailed and, as expected, the boundary-layer thickness increased with increased nozzle-pressure ratio. For the case of a partially boattailed afterbody the boundary-layer thickness remained unchanged with varying nozzle-pressure ratio.



## Jet Spreading Characteristics

The first part of the discussion will cover the runs with convergent nozzles in which most of the data were taken; the remainder will be concerned with convergent-divergent nozzles.

Convergent nozzles. - Ideally, a jet discharging from the base of a body of revolution at zero angle of attack would be circular at all stations downstream of the nozzle exit. A single temperature profile measured in the center-line plane of the jet would thus be sufficient to define the jet at any given station downstream of the nozzle. It was felt, however, in the investigation described herein, that the strut which supported the model in the tunnel created sufficient disturbance to invalidate such a simple procedure as the measurement of a single profile. Consequently, a survey was made in which several lateral profiles were obtained. Typical temperature profiles obtained in this manner at a station 6 nozzle diameters downstream of the nozzle exit are shown in figure 7(a). Cross plots of the lateral profiles which yield mean isotherms are given in figure 7(b). From these curves it is possible to obtain average radii for the various values of $\theta$ and then to construct a mean-temperature profile which is more representative of the actual jet without external disturbances. This method of obtaining mean-temperature profiles was employed with all jet-spreading data.

The mean-temperature profiles of a jet expanding from a convergent nozzle into a moving stream at a Mach number of 1.91 are presented in figure 8. The general similarity at any axial station of the profiles of mixing at various pressure ratios is evident. Increasing the pressure ratio resulted in an increase in jet size with the maximum jet diameter occurring at approximately 2 nozzle diameters downstream of the nozzle exit. Farther downstream the size of the jet decreased slightly. Included in the figure are profiles obtained with the jet expanding into quiescent air to illustrate the marked effect of the external stream in reducing the size of the jet wake. The data presented are for an afterbody having an annular base ($D_b/D_m$, 0.525) and are typical of the data

obtained with all afterbodies investigated. The profiles are given for a range of nozzle-pressure ratios and for several axial stations.

The effect of the external stream is greatest near the edge of the jet. At an axial station of 2 diameters and for a temperature parameter $\theta$ of 0.5, for example, the reduction in jet size due to the influence of the external flow is approximately 20 percent. Near the boundary of the jet, for example, $\theta = 0.1$, the reduction in jet size at 2 diameters is about 30 percent. This phenomenon occurs at all downstream stations with the deviations growing larger with axial distance. A comparison of the temperature profiles (fig. 9) of a jet expanding into a supersonic air stream with those of a jet expanding into quiescent air showed a considerable decrease in jet size for the jet in a moving stream. This decrease ranged from approximately 37 percent at an axial station of 1 diameter downstream of the nozzle exit to more than 55 percent at 8 diameters for the temperature profiles near the jet boundary ($\theta = 0.1$). The difference observed between the quiescent- and moving-air data are to be expected for two reasons: (1) The effective pressure ratio, that is, the ratio of nozzle total pressure to the static pressure in the immediate vicinity of the nozzle exit is considerably less for the jet in the supersonic stream than for the jet expanding into quiescent air because of the strong trailing shock at the nozzle exit; (2) furthermore, the decrease in relative motion between the jet and the moving stream results in a substantial decrease in the jet mixing. These two effects, which were evident in the profiles of figure 8, are emphasized in figure 9, in which the radius of each of the $\theta = 0.1$ and $\theta = 0.5$ isotherms is given as a function of axial distance for a jet in quiescent and in moving air. The decreased difference between the isotherms of $\theta = 0.1$ and $\theta = 0.5$ in the case of the jet with a moving external stream is indicative of the decreased mixing. The inward displacement of the isotherm of $\theta = 0.5$ from the quiescent-air case, particularly near the nozzle exit, is indicative of the effect of the trailing shock wave in decreasing the effective pressure ratio. (It must be stated that the quiescent-air data presented herein are not in exact agreement with the data of reference 2. Presumably this is a result of the different environmental conditions wherein one jet discharged into a tank, and the other discharged into the tunnel test section, thus creating different secondary flows.)

The effective nozzle-pressure ratio may be defined for convenience as the ratio of the nozzle total pressure to the static pressure immediately after the trailing oblique external shock wave in the vicinity of the nozzle edge. The static pressure at the jet boundary decreases with increasing distance downstream so that the effective nozzle-pressure ratio so defined is of qualitative value only. In the case of the nozzle with a 5.63° boattail terminating with a sharp nozzle edge, an effective nozzle-pressure ratio of 4.35 was estimated to correspond to an actual nozzle-pressure ratio of 10 in the present runs. This value

of 4.35 is sufficiently close for an approximate comparison with a jet expanding into quiescent air at a nozzle-pressure ratio of 4.60. This comparison is made in figure 10, in which the isotherms of $\theta = 0.1$ and $\theta = 0.5$ are given for both jets. For both values of $\theta$ there is fair agreement near the nozzle exit and for the case of $\theta = 0.5$ the agreement is fair for the entire range investigated. The deviation between lines of $\theta = 0.1$ for a jet in quiescent and moving air at stations more than 2 or 3 nozzle diameters downstream again serves to illustrate the pronounced effect of reduced mixing on jet size.



Schlieren photographs of the jet at various pressure ratios in quiescent air and moving air are compared in figure 11. The effects of the external stream are readily apparent.

In order to determine the effect of afterbody geometry on jet spreading, surveys were made of jets discharging from partially and completely boattailed afterbodies having boattail angles of $5.63^\circ$ and $9.33^\circ$. The results of this study are given in figure 12, in which lines of $\theta = 0.1$ are given as functions of axial distance for four different nozzle exits. Comparison of the contours for two partially boattailed bodies with different boattail angles shows very good agreement for all downstream stations. There was also good agreement for the other values of $\theta$ although the data are not given here. For the range investigated, the size of the boattail angles thus had no effect on jet spreading. A comparison of the boundaries of $\theta = 0.1$ for the partially and completely boattailed afterbodies indicates a slightly larger jet for the partially boattailed nozzle. This is probably due to the fact that in the case of the completely boattailed nozzle the expanding jet causes an immediate deflection of the free-stream flow with a resultant increase in static pressure in the vicinity of the nozzle exit; whereas in the case of the partially boattailed nozzle the expanding jet does not cause a flow deflection immediately at the nozzle exit, but rather at some finite distance downstream. The effect of boattailing on jet spreading is also shown in figure 13 in which schlieren photographs for a boattail with and without annulus illustrate the higher initial expansion angle with the annulus and the appreciably different shock patterns in the jet.

Convergent-divergent nozzles. - A knowledge of the growth and decay of jets expanding from convergent-divergent as well as from convergent nozzles is of interest. The amount of overpressure with which the jet is expanding both in quiescent air and in a moving stream has been shown to be a prime parameter in determining the amount of jet spreading. Thus, for purposes of comparison with jet-spreading data obtained with a convergent nozzle, two convergent-divergent nozzles were operated at approximately the same degree of overpressure (that is, the same ratio of nozzle-exit static pressure to ambient pressure). The internal geometry for both nozzles was the same with a design nozzle-pressure ratio of 10.5. The only difference between nozzles was the extent of external boattailing;

one nozzle was completely boattailed ($D_b/D_m = 0.385$) and the other had an annular base ($D_b/D_m = 0.525$). The nozzles were operated at pressure ratios of 24.34 and 13.22, values which gave degrees of overpressure comparable with those obtained with the convergent nozzles operated at pressure ratios of 4.6 and 2.5. The results of the investigation shown in figure 14 agree with the observation made from the convergent-nozzle studies, that is, the effect of completely boattailing the afterbody is to reduce the size of the jet.

A comparison of the jet boundary for a convergent nozzle with that for a convergent-divergent nozzle having approximately the same degree of overpressure (fig. 15) gives results similar to those reported in reference 3, in that the boundary for the jet from a convergent-divergent nozzle is slightly larger because of the larger potential core in the jet. Also shown in figure 15 is the boundary for a jet expanding from a convergent-divergent nozzle into quiescent air (taken from reference 3). The design nozzle-pressure ratio for the convergent nozzle is 4.6 and the boundary presented is for a jet operated at the same degree of overpressure as the other jets represented. Although the boundary for the jet in quiescent air is defined by a Mach number ratio of 0.10 rather than by a temperature line of $\theta = 0.1$, it is believed sufficiently close to the temperature boundary for comparison purposes (see reference 2). Apparently the variation between jets expanding from convergent-divergent nozzles into quiescent air and into a moving air stream is similar to that between jets expanding from convergent nozzles; a much smaller jet is obtained for the case of the moving stream.

The schlieren photographs of figure 16, in which jets expanding from convergent nozzles are compared with those expanding from convergent-divergent nozzles at approximately the same overpressure ratio, show the variation in the potential core as evidenced by the change in shock structure.



## SUMMARY OF RESULTS

From temperature surveys of jets expanding from choked nozzles into a stream of Mach number 1.91, the following results were obtained:

1. The effect of nozzle-pressure ratio on jet spreading, as in the case of quiescent air, was significant. Increasing the pressure ratio resulted in an increase in jet size with the maximum jet diameter occurring at approximately 2 nozzle diameters downstream of the nozzle exit. Farther downstream the size of the jet decreased slightly.

2. The temperature profiles for a jet expanding into a moving stream were smaller than those for a jet expanding into quiescent air by approximately 37 percent at an axial station of 1 diameter downstream of the

nozzle exit and more than 55 percent at an axial station of 8 diameters. The difference in jet size resulted from the fact that (1) The effective pressure ratio, that is, the ratio of nozzle total pressure to the static pressure in the immediate vicinity of the nozzle exit was much lower than the actual nozzle-pressure ratio, and (2) the reduction in relative motion between the jet and the moving stream tended to reduce the mixing and thus made the jet smaller.



3. Changing the afterbody geometry from a completely to a partially boattailed nozzle resulted in a slight increase in the jet size. Variation of boattail angle in the range investigated had no effect on jet spreading.

4. The jet-temperature profiles for the convergent-divergent nozzle were somewhat larger than those for the convergent nozzle with both types operating at the same overpressure ratio. This was accounted for by the fact that the potential core in the jet expanding from the convergent-divergent nozzle was larger.

Lewis Flight Propulsion Laboratory
National Advisory Committee for Aeronautics
Cleveland, Ohio

## REFERENCES

1. Sloop, John L., and Morrell, Gerald: Temperature Survey of the Wake of Two Closely Located Parallel Jets. NACA RM E9I21, 1950.

2. Rousso, Morris D., and Kochendorfer, Fred D.: Velocity and Temperature Fields in Circular Jet Expanding from Choked Nozzle into Quiescent Air. NACA RM E51F18, 1951.

3. Rousso, Morris D., and Kochendorfer, Fred D.: Experimental Investigation of Spreading Characteristics of Choked Jets Expanding into Quiescent Air. NACA RM E50E03a, 1950.

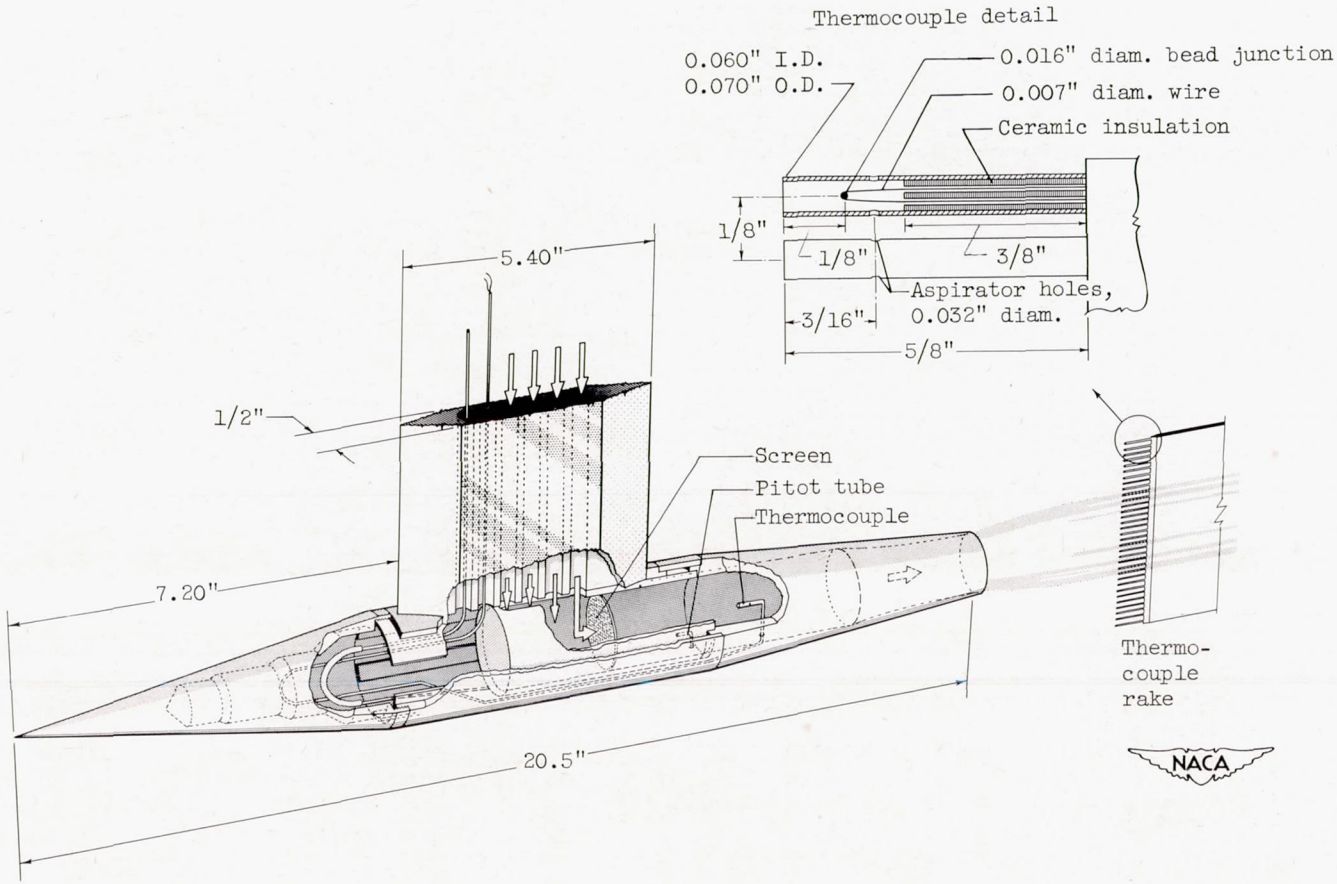


Figure 1. - Sketch of model and support showing internal instrumentation and traversing thermocouple rake.

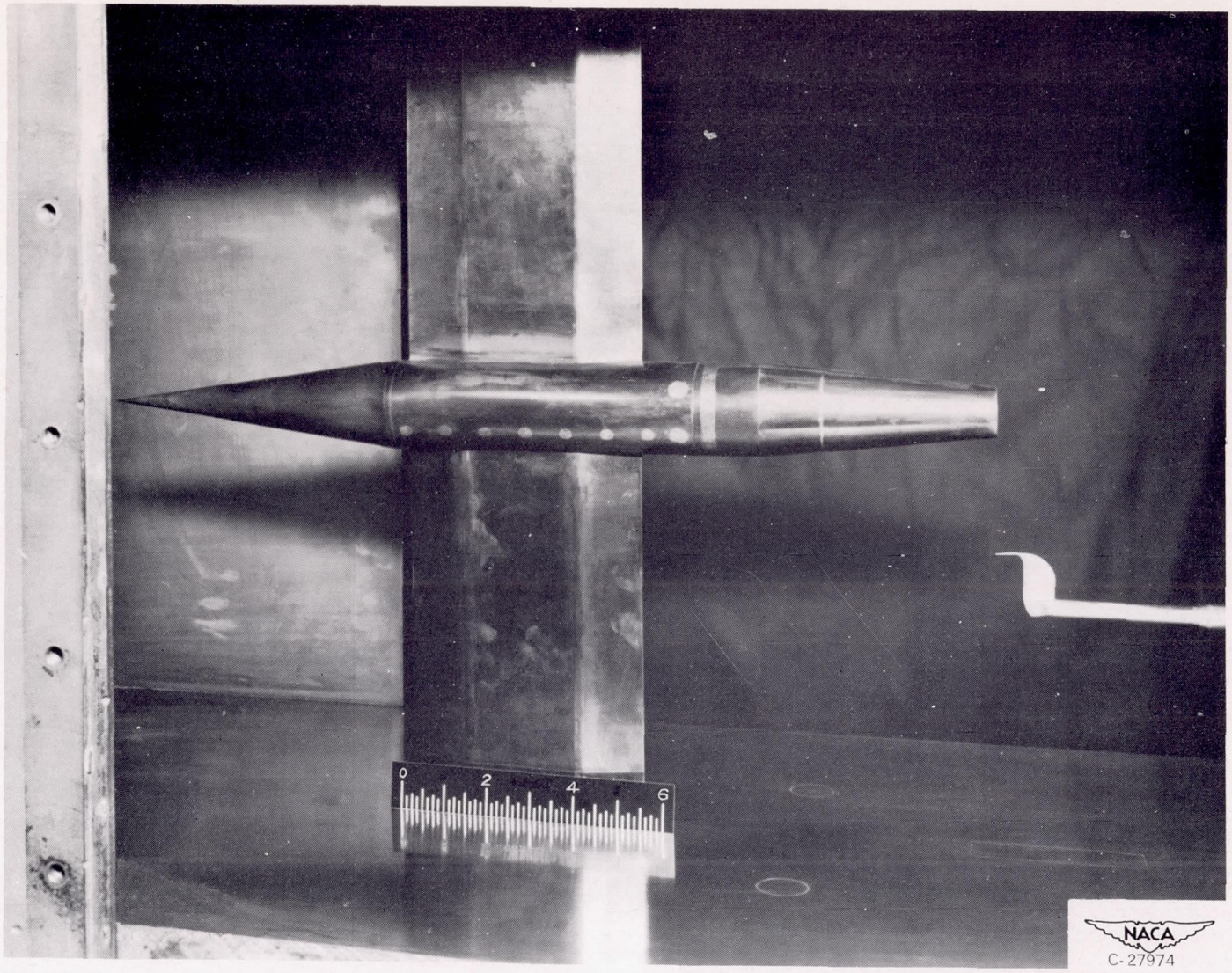


Figure 2. - Photograph of model with double strut in 18- by 18-inch supersonic wind tunnel showing boundary-layer probe. (Scale given in inches.)

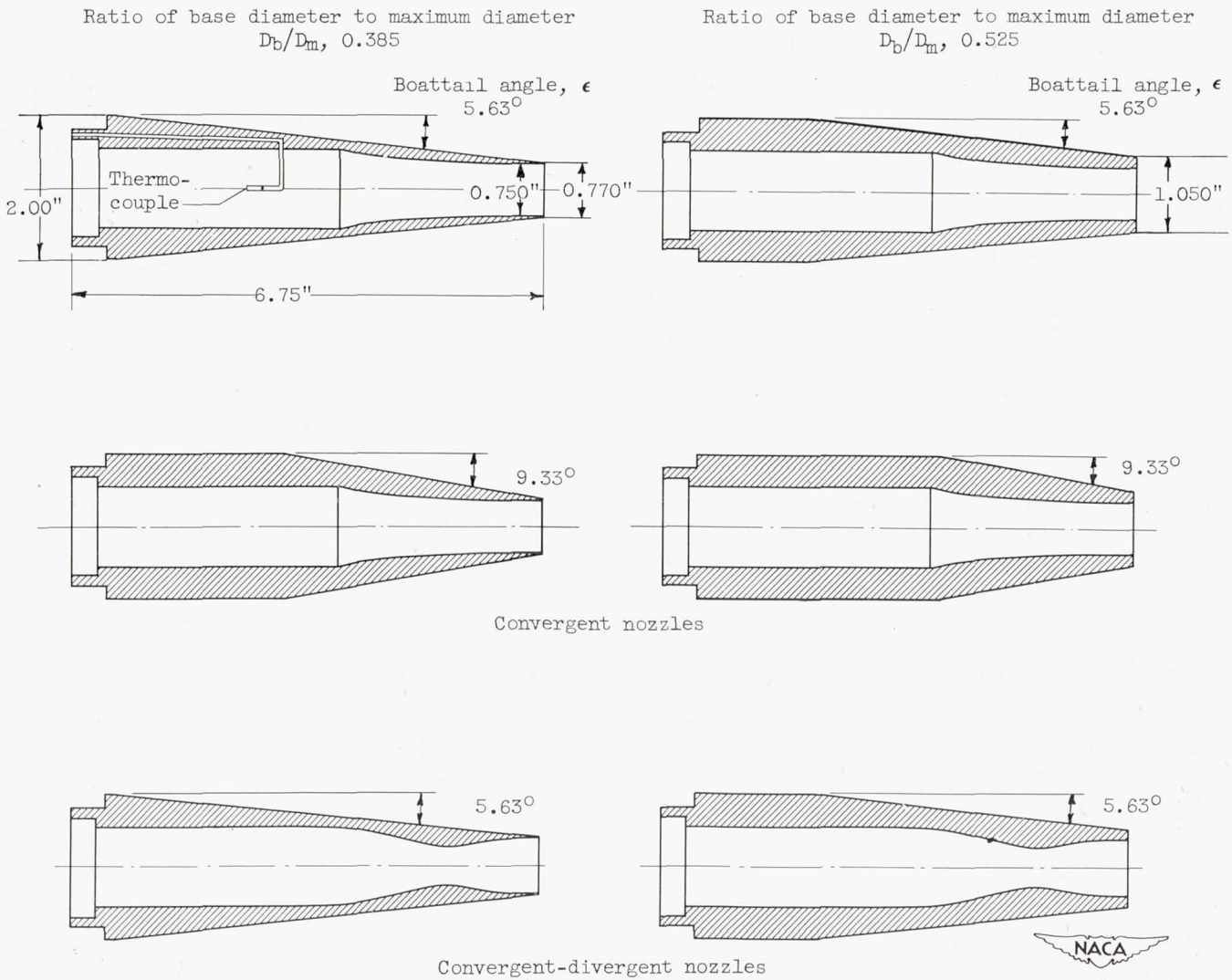


Figure 3. - Sketch of afterbody configurations investigated showing location of thermocouple.

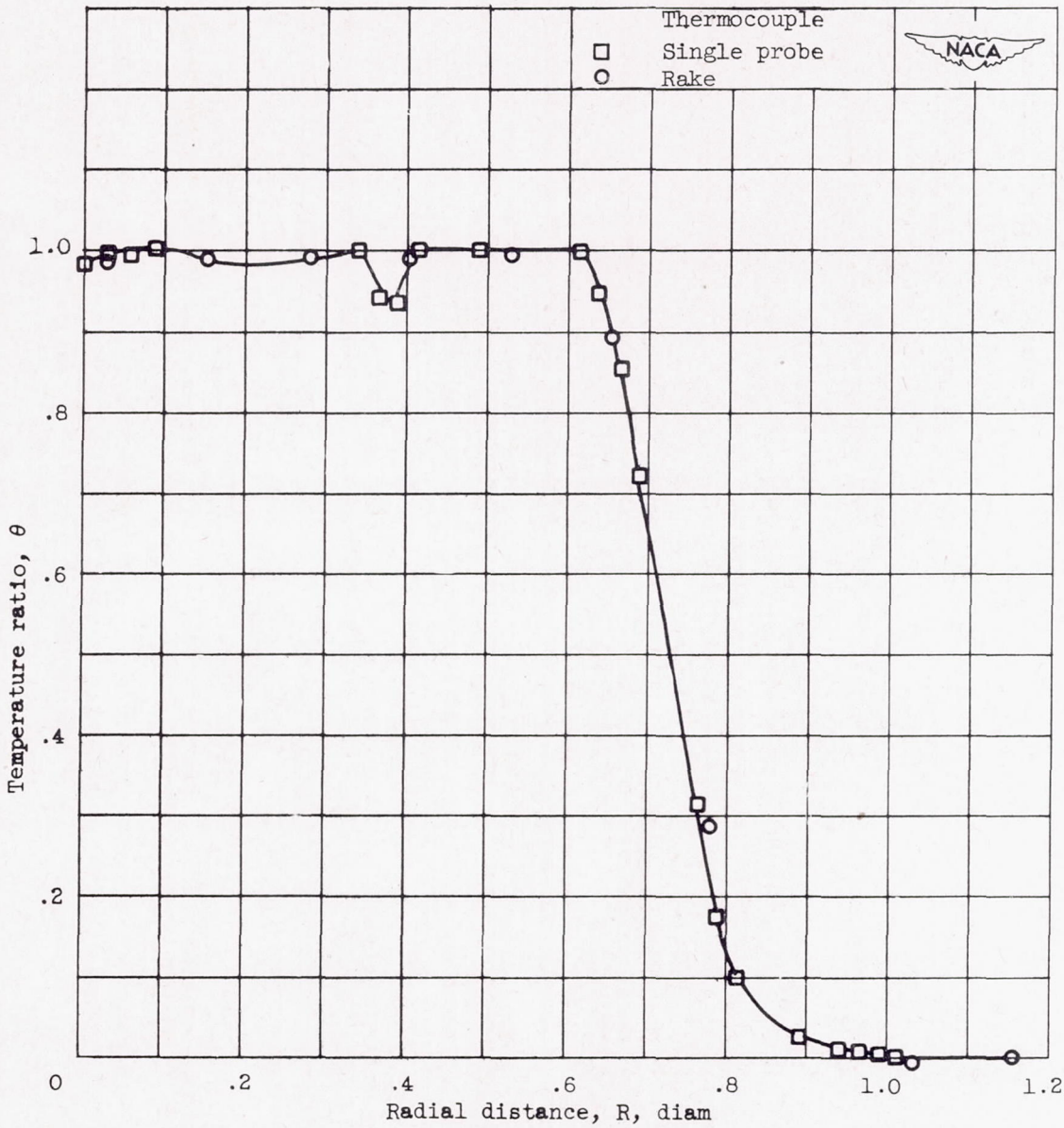


Figure 4. - Comparison of temperature profiles in heated jet as determined by single- and multiple-thermocouple probes. Nozzle-pressure ratio, 16.0; axial distance downstream of nozzle exit, 2 diameters.

Single strut

NACA
C-28648

Double strut

Figure 5. - Comparison of jet expanding from model having single strut with jet expanding from model having double strut.

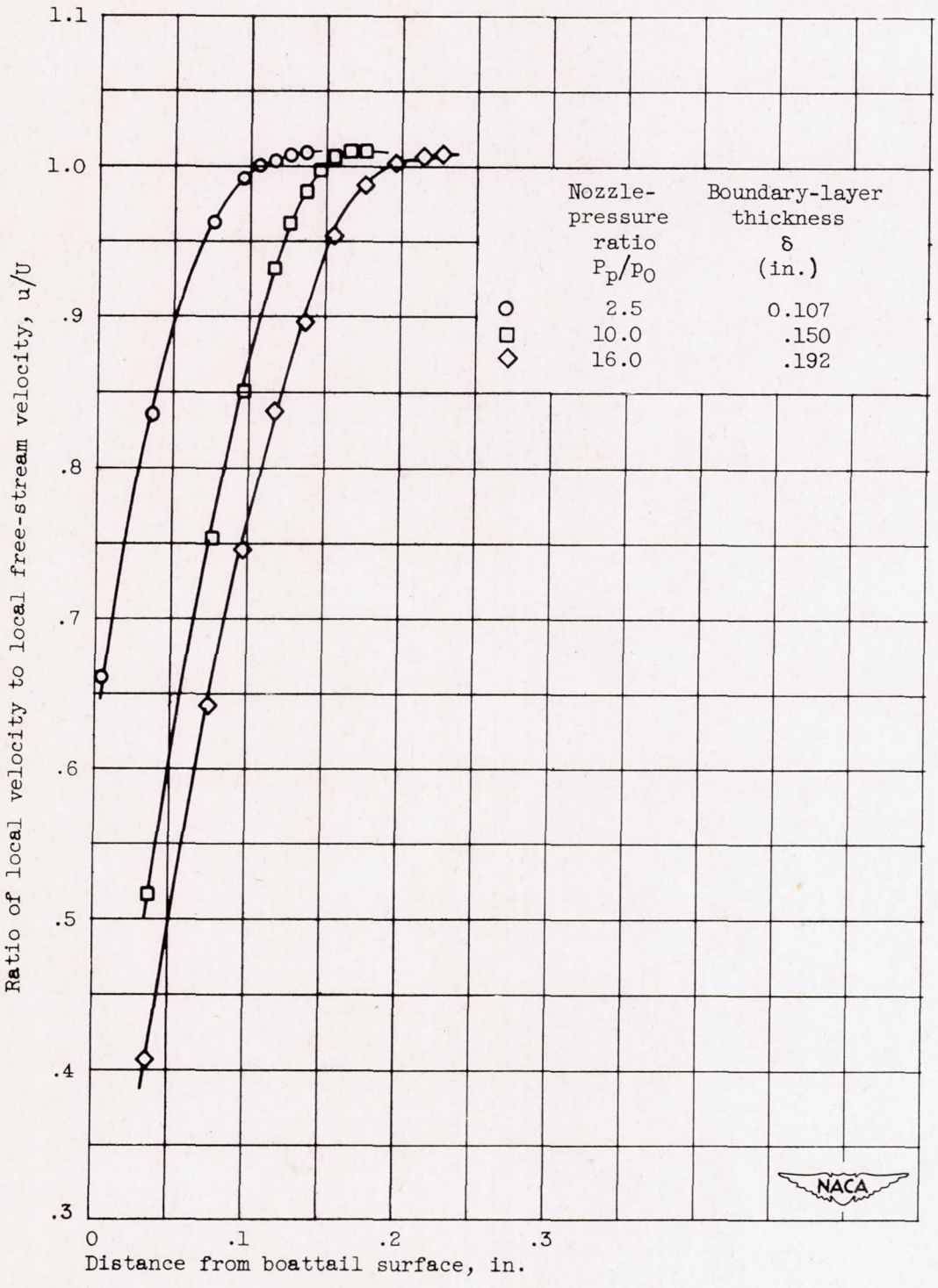


Figure 6. - Velocity profiles at boattail exit for jet expanding at several nozzle-pressure ratios. Convergent nozzle; ratio of base diameter to maximum diamter, 0.385; boattail angle, 9.33°.

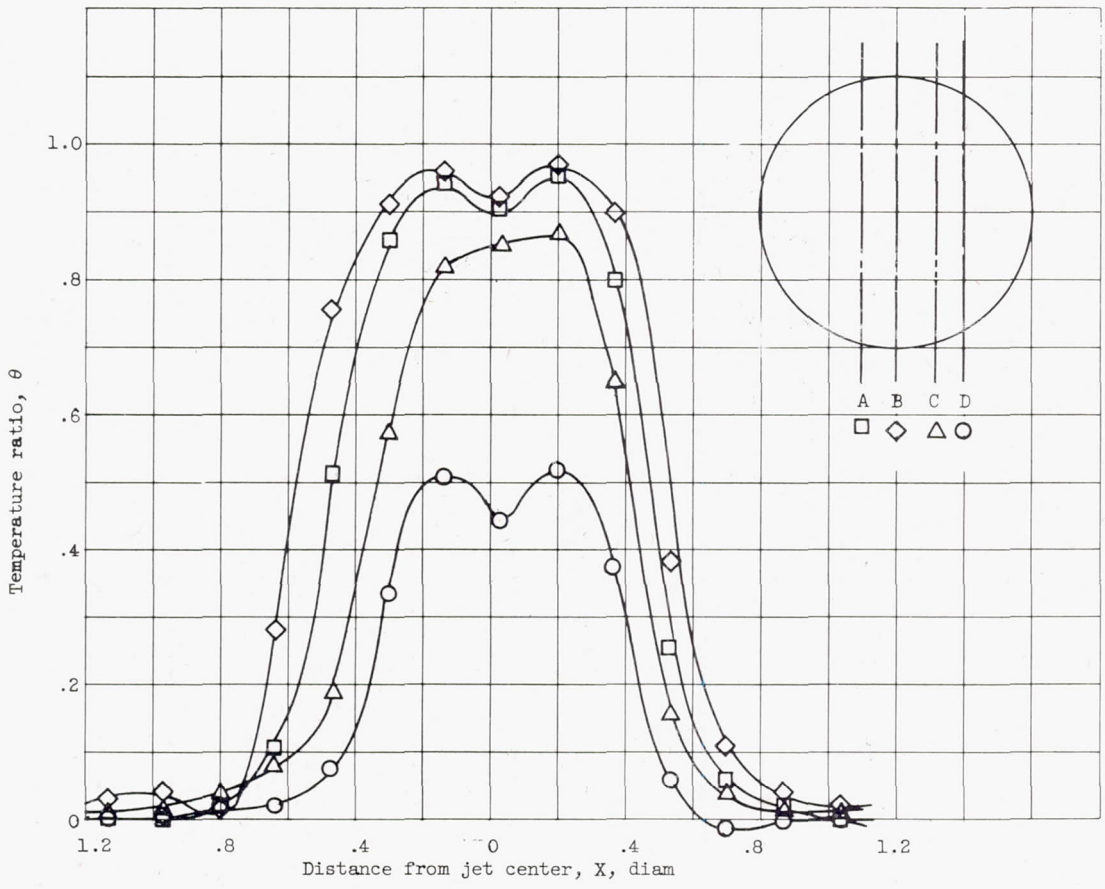


(a) Measurements at four lateral positions in heated jet.

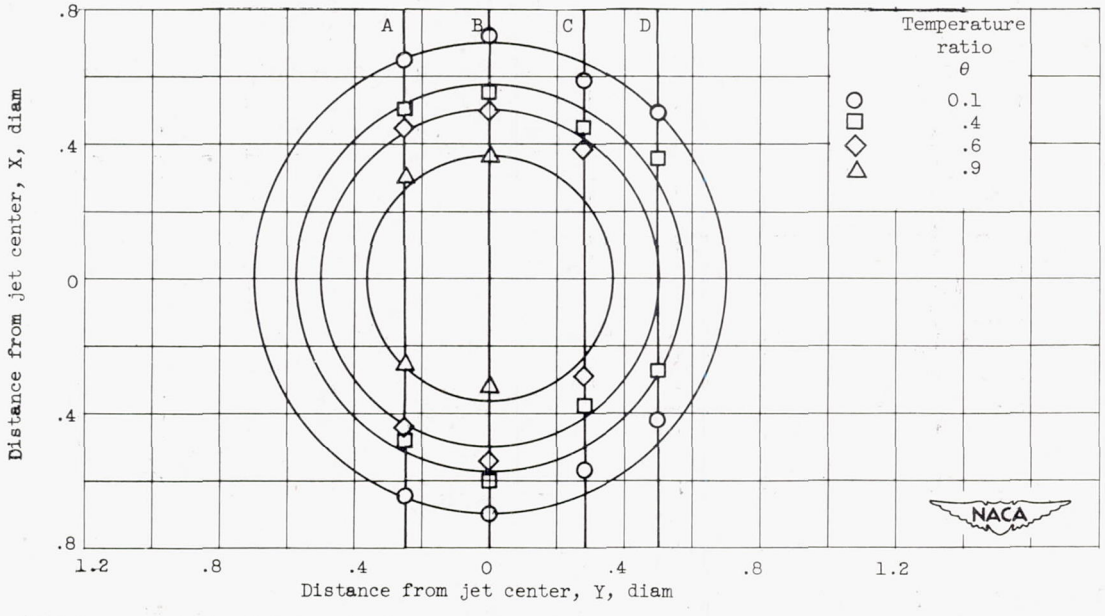


(b) Cross plot showing mean isotherms used to determine mean-temperature profile.

Figure 7. - Temperature profiles. Axial distance downstream of nozzle exit, 6 diameters; nozzle-pressure ratio, 4.6.

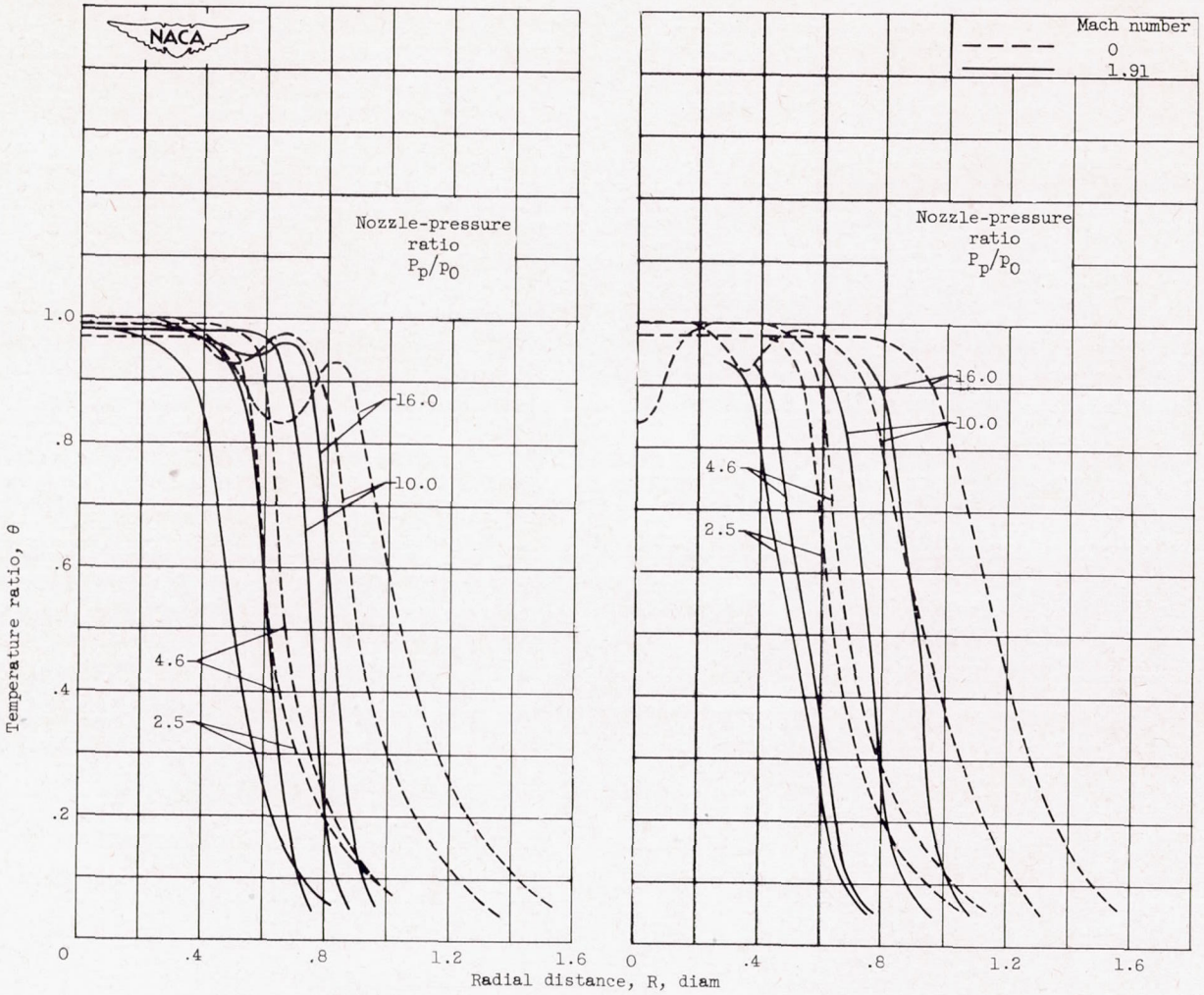


(a) Axial distance downstream of nozzle exit, 1 diameter.

(b) Axial distance downstream of nozzle exit, 2 diameters.

Figure 8. - Temperature profiles in heated jet expanding from a convergent nozzle. Nozzle-inlet temperature, 300° F; ratio of base diameter to maximum diameter, 0.525; boattail angle, 5.63°.

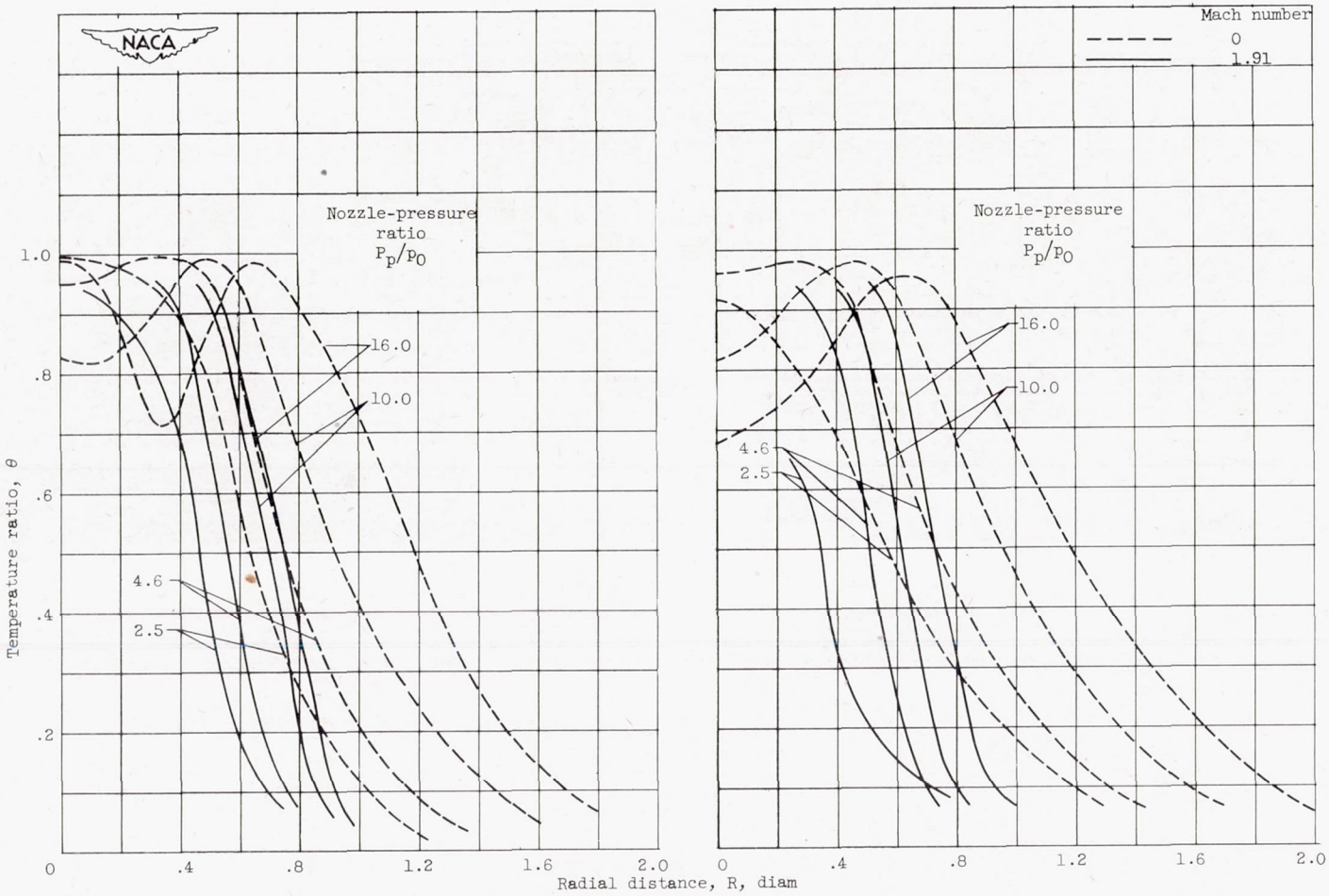


(c) Axial distance downstream of nozzle exit, 4 diameters.

(d) Axial distance downstream of nozzle exit, 6 diameters.

Figure 8. - Continued. Temperature profiles in heated jet expanding from a convergent nozzle. Nozzle-inlet temperature, 300° F; ratio of base diameter to maximum diameter, 0.525; boattail angle, 5.63°.

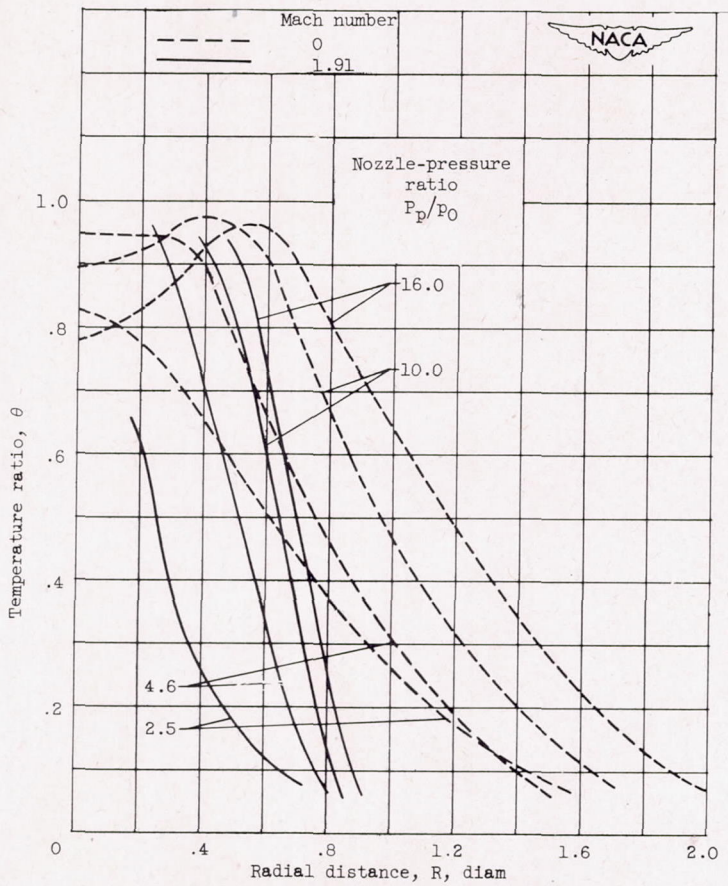


(e) Axial distance downstream of nozzle exit, 8 diameters.

Figure 8. - Concluded. Temperature profiles in heated jet expanding from a convergent nozzle. Nozzle-inlet temperature, 300° F; ratio of base diameter to maximum diameter, 0.525; boattail angle, 5.63°.

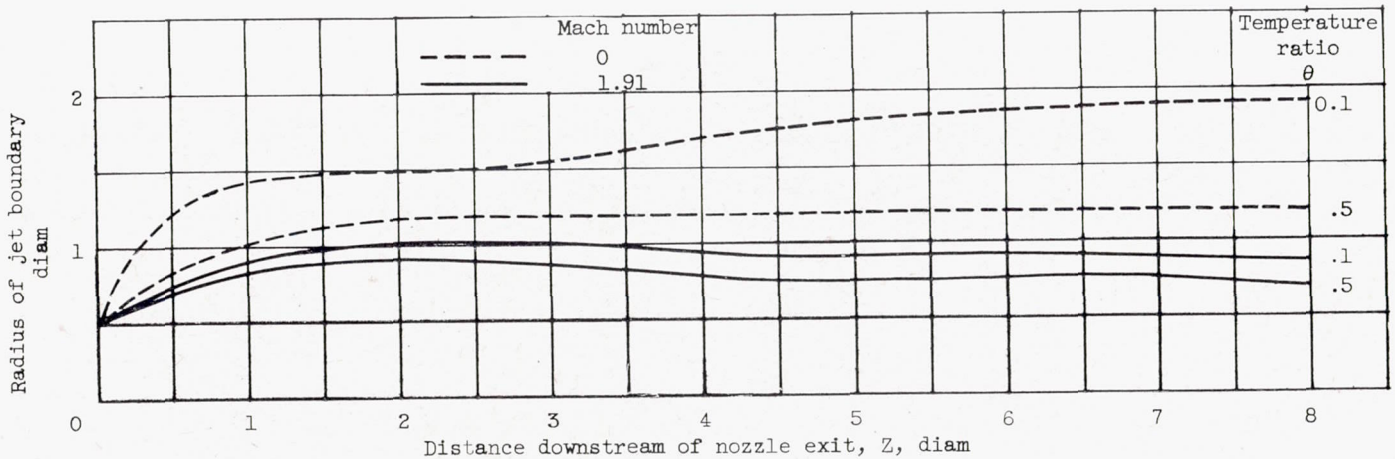


Figure 9. - Isotherms of jet expanding from convergent nozzle into quiescent air and into moving stream. Ratio of base diameter to maximum diameter, 0.525; boattail angle, 5.63°; nozzle-pressure ratio, 16.0.

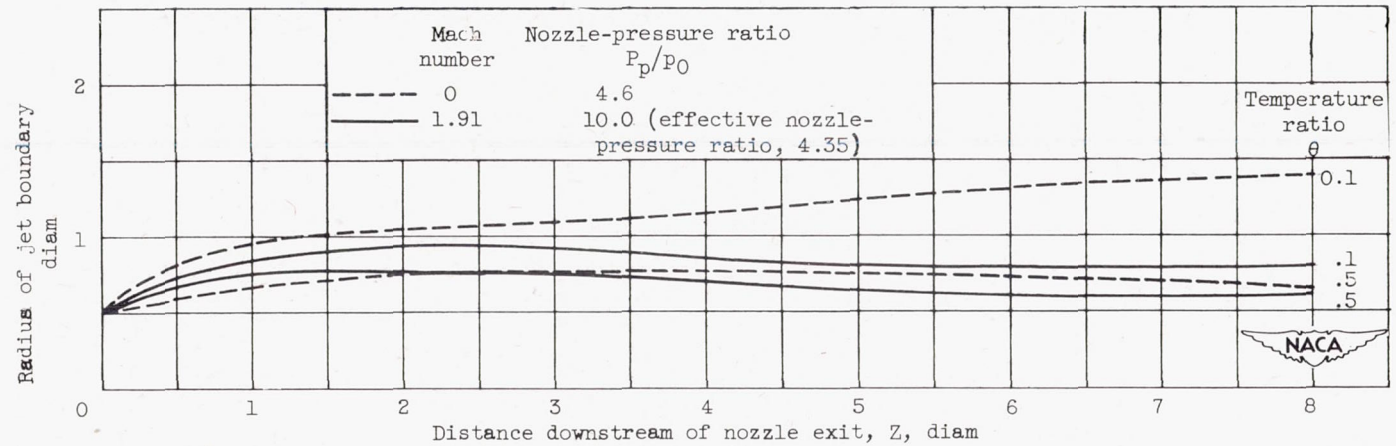


Figure 10. - Comparison of isotherms of $\theta = 0.1$ and $\theta = 0.5$ of jet in quiescent air and jet with approximately the same effective pressure ratio in moving stream. Ratio of base diameter to maximum diameter, 0.525; boattail angle, 5.63°.

Mach number, $M_0$, 0

Mach number, $M_0$, 1.91

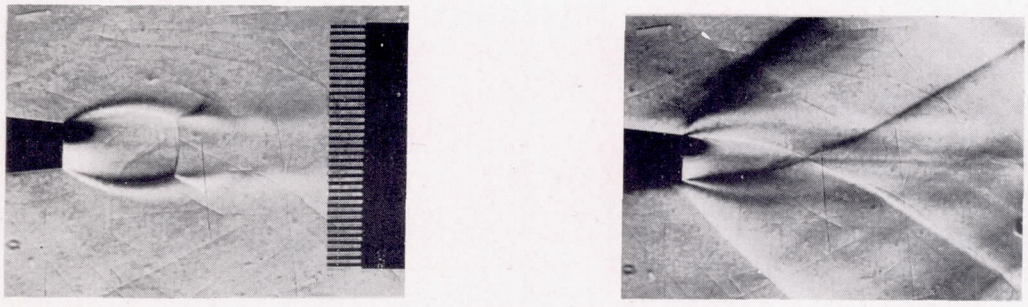

Nozzle-pressure ratio, $P_p/p_0$, 16.0

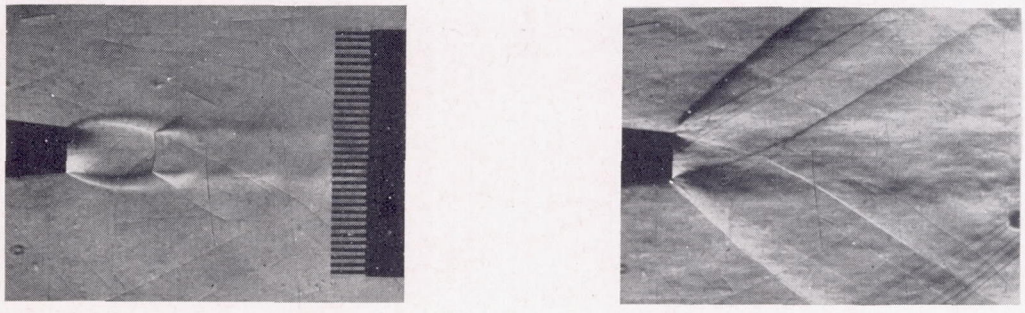

Nozzle-pressure ratio, $P_p/p_0$, 10.0

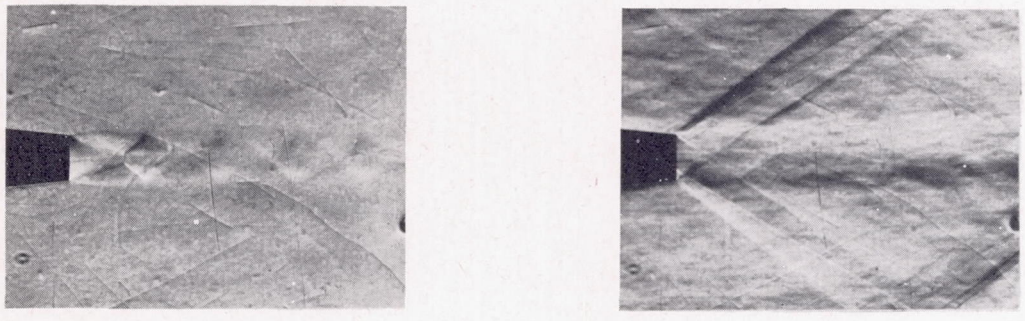

Nozzle-pressure ratio, $P_p/p_0$, 4.6

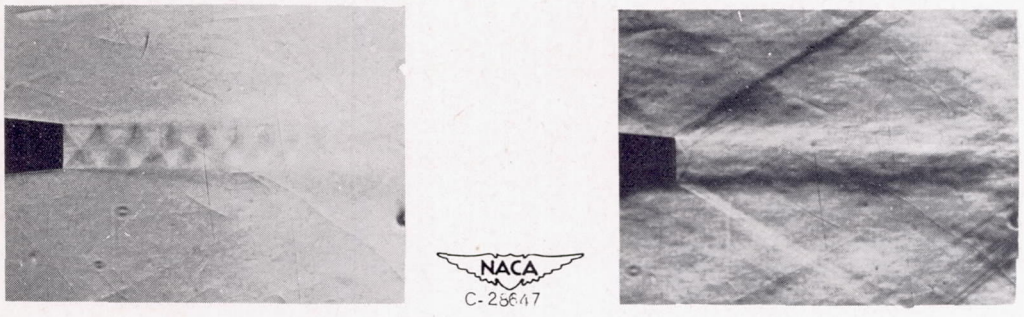



Nozzle-pressure ratio, $P_p/p_0$, 2.5

Figure 11. - Comparison of jets expanding from convergent nozzles into quiescent air and into moving stream. Ratio of base diameter to maximum diameter, 0.385; boattail angle, 5.63°.

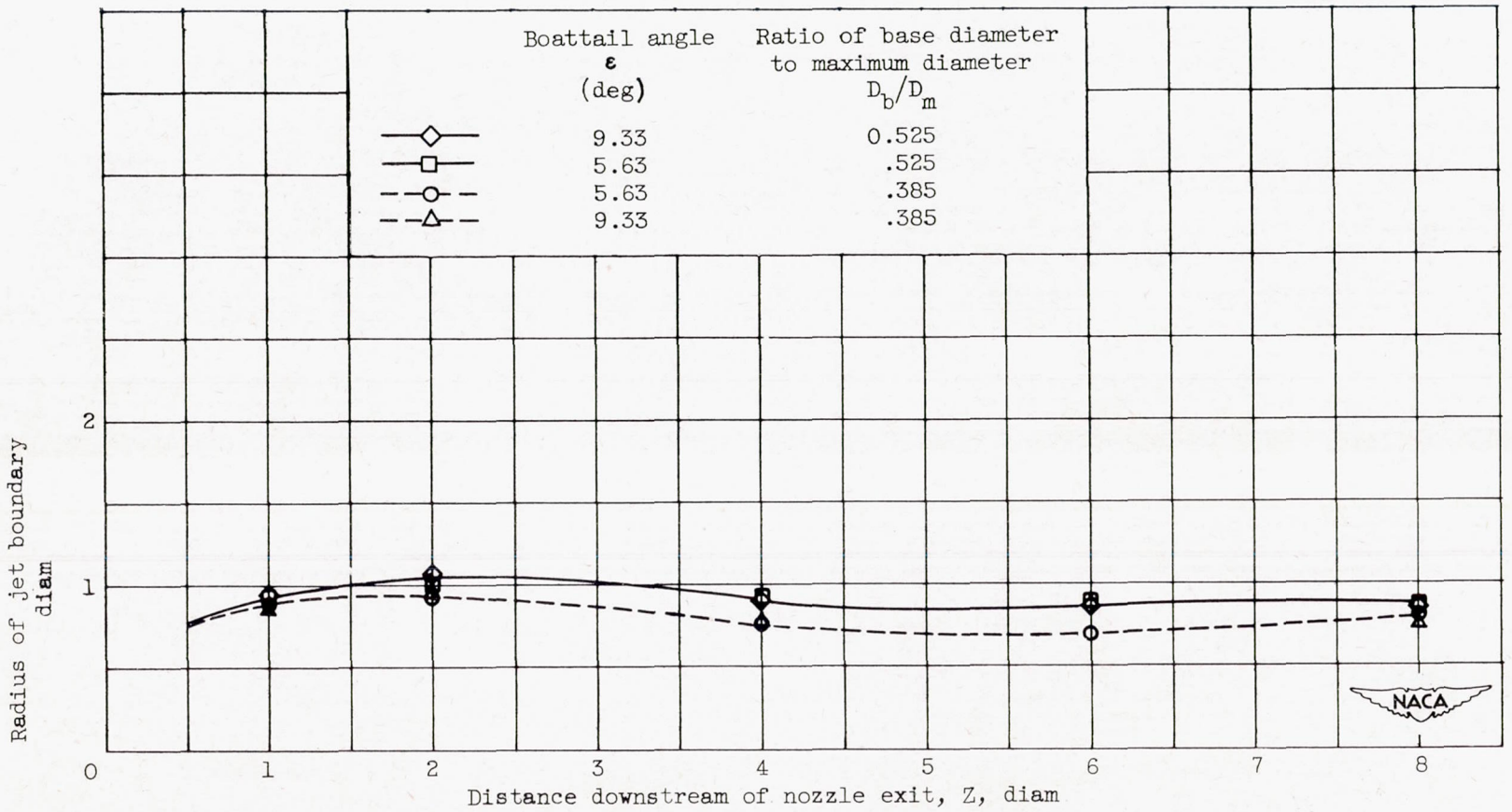


Figure 12. - Spreading of jet expanding from convergent nozzle into moving stream. Temperature ratio, 0.1.

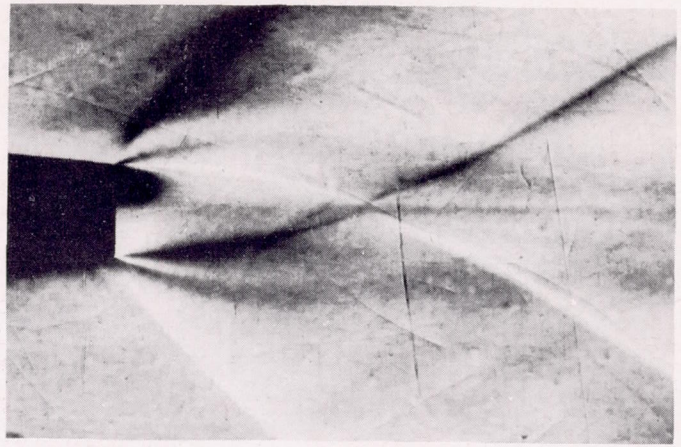

(a) Ratio of base diameter to maximum diameter, 0.385; nozzle-pressure ratio, 16.0.

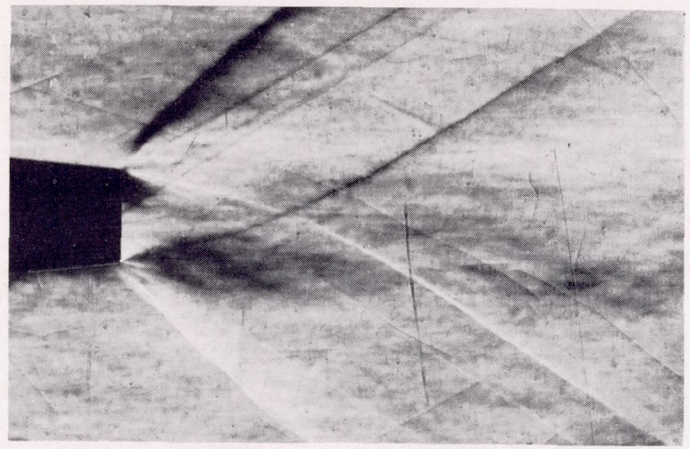

(b) Ratio of base diameter to maximum diameter, 0.385; nozzle-pressure ratio, 10.0.

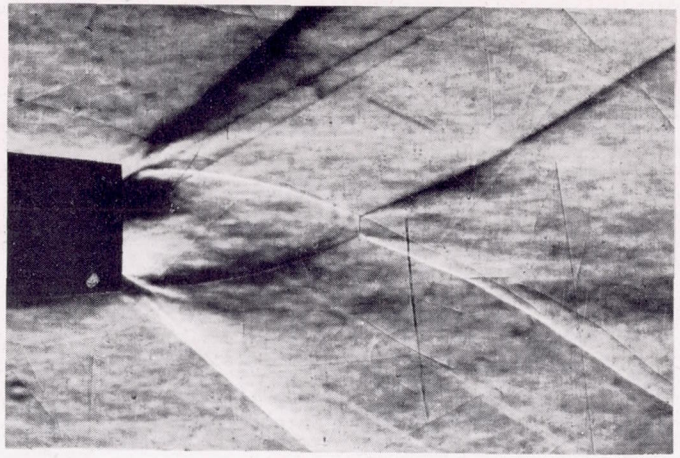

(c) Ratio of base diameter to maximum diameter, 0.525; nozzle-pressure ratio, 16.0.

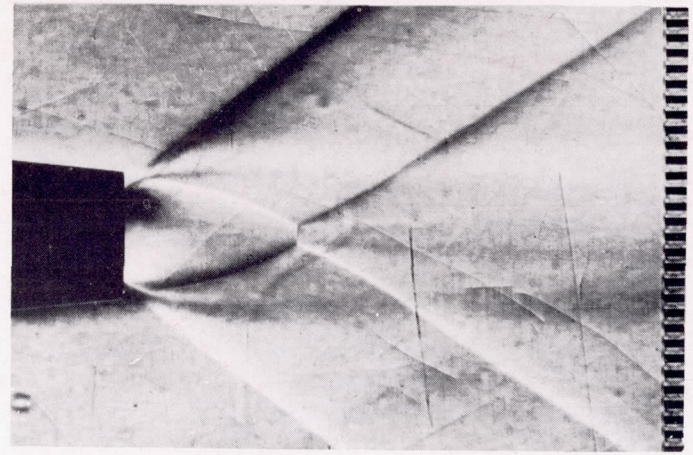

(d) Ratio of base diameter to maximum diameter, 0.525; nozzle-pressure ratio, 10.0.

NACA
C-28646

Figure 13. - Comparison of jets expanding from partially and completely boattailed convergent nozzles. Boattail angle, 5.63°.

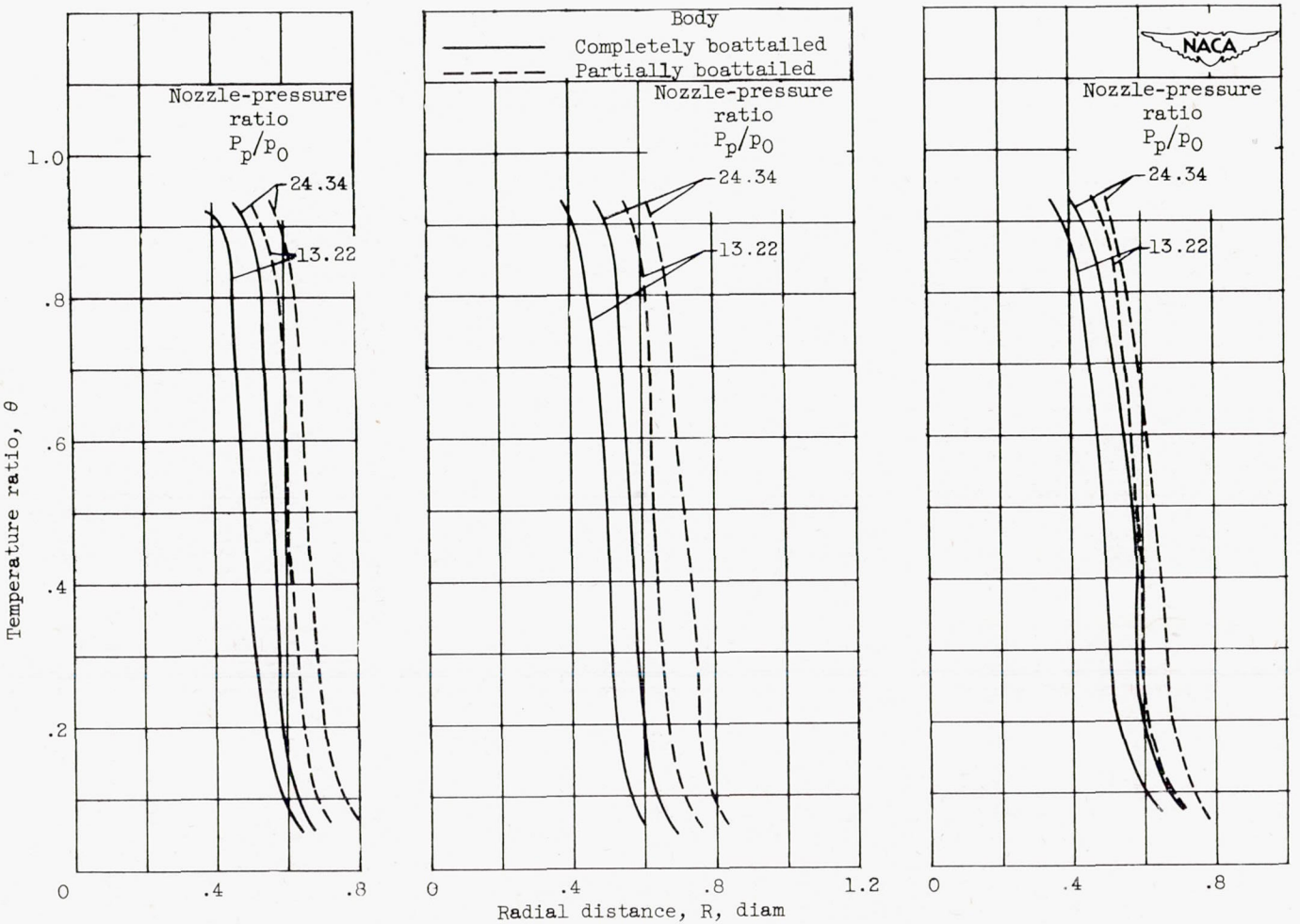


(a) Axial distance downstream of nozzle exit, 1 diameter.

(b) Axial distance downstream of nozzle exit, 2 diameters.

(c) Axial distance downstream of nozzle exit, 4 diameters.

Figure 14. - Temperature profiles in jet expanding from partially and completely boattailed bodies with convergent-divergent nozzles. Boattail angle, 5.63°.

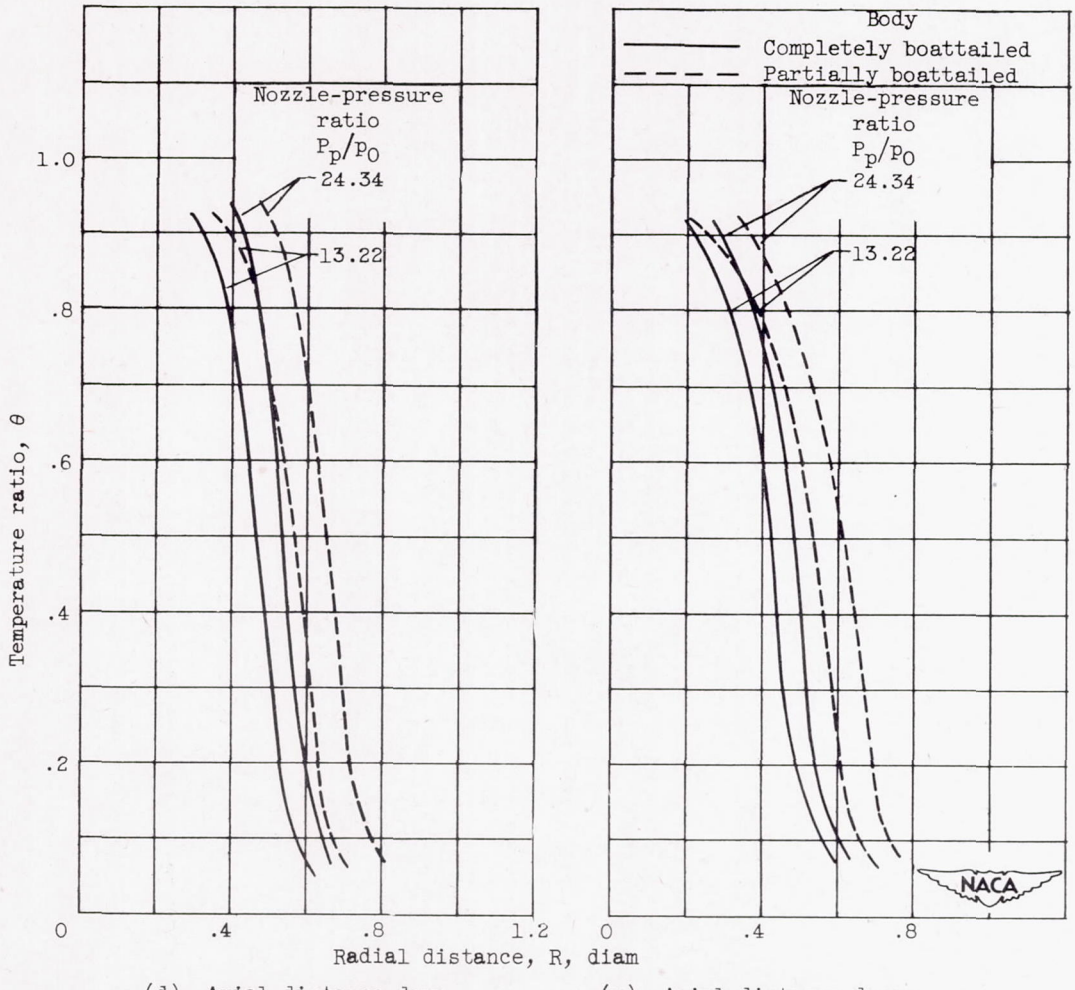


(d) Axial distance downstream of nozzle exit, 6 diameters.

(e) Axial distance downstream of nozzle exit, 8 diameters.

Figure 14. - Concluded. Temperature profiles in jet expanding from partially and completely boattailed bodies with convergent-divergent nozzles. Boattail angle, 5.63°.

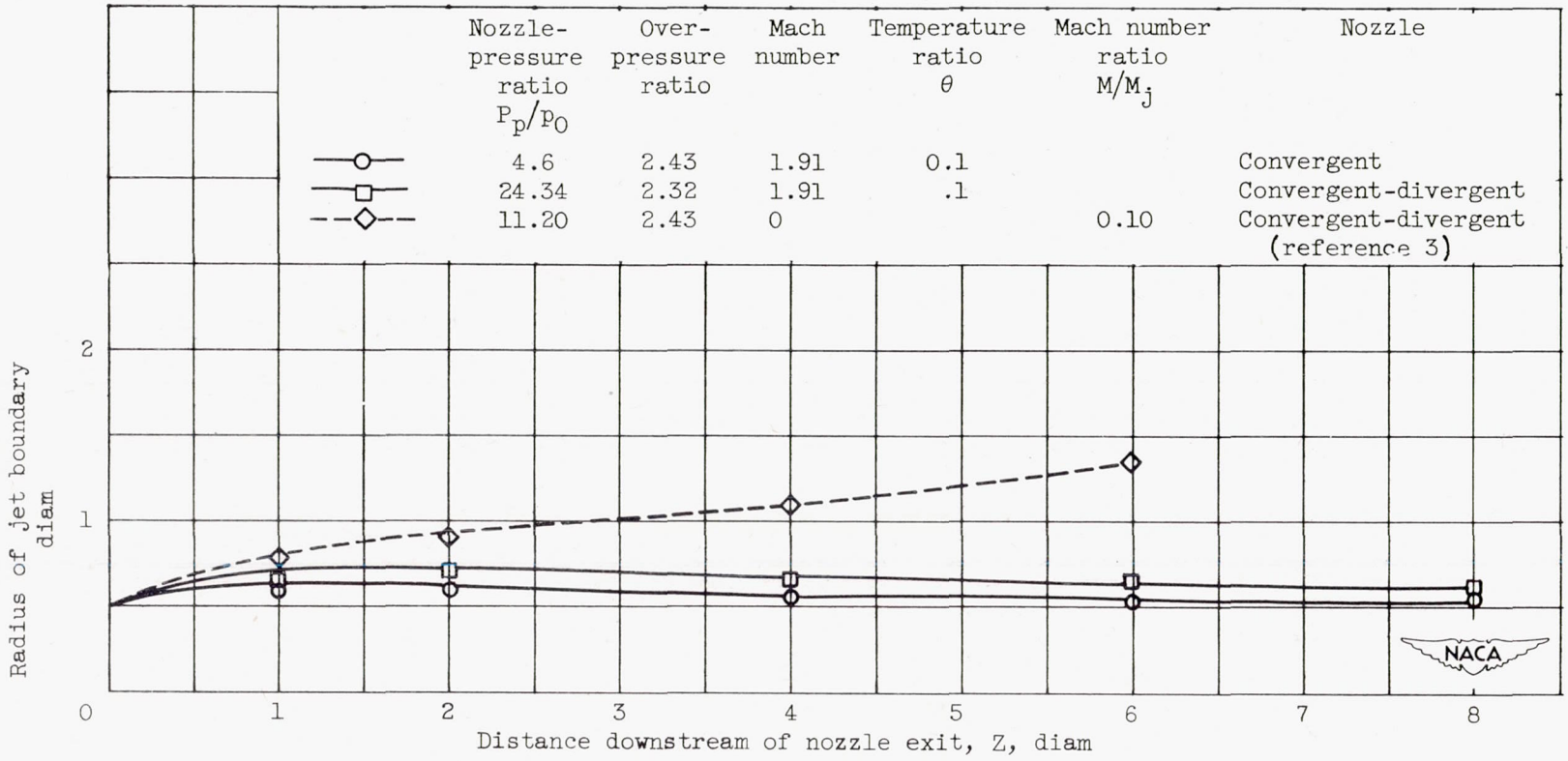


Figure 15. - Spreading of jet expanding from convergent and convergent-divergent nozzles.

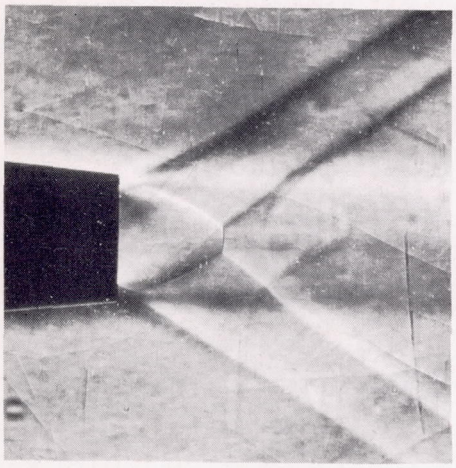

(a) Convergent nozzle. Nozzle-pressure ratio, 4.6.

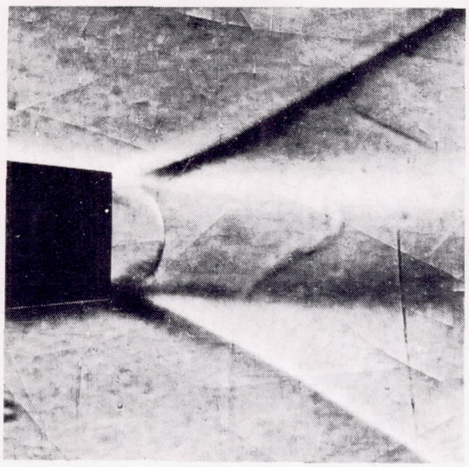

(b) Convergent nozzle. Nozzle-pressure ratio, 2.5.

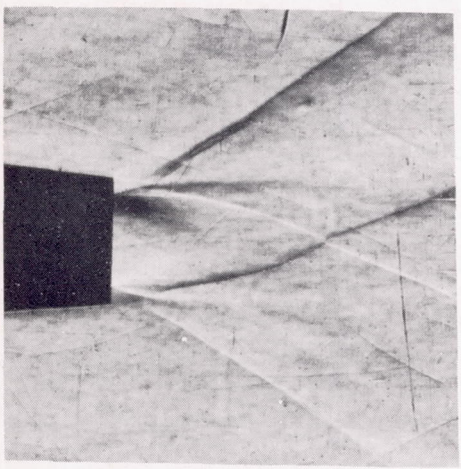

(c) Convergent-divergent nozzle. Nozzle-pressure ratio, 24.34.

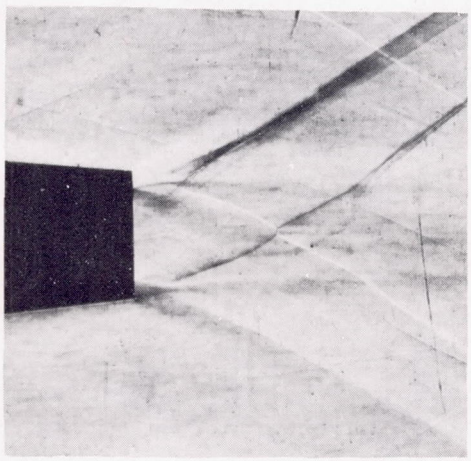

(d) Convergent-divergent nozzle. Nozzle-pressure ratio, 13.22.

C-28649

Figure 16. - Comparison of jets expanding from convergent and convergent-divergent nozzles. Ratio of base diameter to maximum body diameter, 0.525; boattail angle, 5.63°.



NACA-Langley - 2-11-52 - 500

CONFIDENTIAL